LuTan-1 Satellite-Based Geological Disaster Detection in Lingbao City, Western Henan of China

Jing Lu[1], Xinming Tang[1], Lei Wei[2], Lingfei Guo[2], Tao Li[1], Xiang Zhang[1], Xuefei Zhang[1]

[1] Land Satellite Remote Sensing Application Center, MNR, Beijing 100048, China
[2] Henan Geological Bureau Mineral Resources Exploration Center, Henan 450016, China

Keywords: Geological Disaster, LT-1, Henan province, DInSAR, SBAS-InSAR.

Abstract

China's monsoon climate makes it prone to geological disasters like landslides, especially from April to October. Henan Province, with 44.3% mountainous and hilly areas, is highly vulnerable, particularly in the western, northern, and southern highlands, northern plains, and eastern areas. These disasters have increased year-round due to climate change and human activities. The L-band Differential Interferometric Synthetic Aperture Radar (LT-1 01 constellation) was successfully launched in early 2022 and is widely applied in geological hazard monitoring. In this paper, a comprehensive deformation survey was conducted in Henan using LT-1 data (3-meter resolution). The process included three stages: deformation survey using D-InSAR on 1,763 high resolution LT-1 scenes (identifying 1,304 deformed areas, with only 158 coinciding with registered disaster points); deformation screening using SBAS on 700 LT-1 scenes; and detailed investigation in Lingbao City, identifying 14 new hazard sites. This paper provides an effective reference for domestic satellites to carry out large-scale geological disaster hazard identification tasks.

1.Introduction

China's monsoon-influenced climate makes it prone to geological disasters[1] like landslides and collapses, especially from April to October due to climate change[2]. Henan Province, with 44.3% of its land being mountainous and hilly, is highly vulnerable, particularly in its western, northern, and southern highlands, as well as the northern plains and eastern areas[3]. Geological disasters in Henan have increased, especially before the flood season (June-September), and now occur year-round due to climate change and human activities. Heavy rainfall and snow-melt significantly raise the risk of debris flows and landslides[4].

The key characteristics of Henan's geological disasters include: occurring mainly in known disaster-prone areas; being concentrated in the flood season; involving mostly small-scale events; being primarily triggered by rainfall, with human activities also playing a role; and consisting mainly of collapses, landslides, and subsidence due to human engineering. From 2011 to 2022, Henan Province experienced nearly 880 geological disasters, resulting in 18 deaths. Currently, there are 2,470 known geological hazard points in Henan Province, threatening 165,200 people and property valued at 6.611 billion yuan.

The L-band Differential Interferometric Synthetic Aperture Radar (LT-1 01 constellation)[5] was successfully launched in early 2022 and has since provided over 400,000 scenes of LT-1 data to domestic natural resources sectors, widely applied in geological hazard monitoring[6]. To ensure effective monitoring and targeted disaster prevention during the flood season, we conducted a comprehensive deformation survey and screening in Henan Province using LT-1 data.

This study utilized LT-1 scenes with 3-meter resolution across Henan Province, complemented by Copernicus Digital Elevation Model (COP-DEM) as external DEM data. At two newly identified hazard sites, drone technology was used to obtain oblique photogrammetry and LiDAR topographic models. The data processing and analysis in Henan Province were divided into three stages: deformation survey, deformation screening, and detailed deformation investigation and measurement, with the sequential application of Differential InSAR (DInSAR), small baseline subset InSAR (*SBAS*-InSAR) and detailed investigation methods.

2.Datasets and methods

2.1 Study area

The key characteristics of Henan's geological disasters include: occurring mainly in known disaster-prone areas; being concentrated in the flood season; involving mostly small-scale events; being primarily triggered by rainfall, with human activities also playing a role; and consisting mainly of collapses, landslides, and subsidence due to human engineering. From 2011 to 2022, Henan Province experienced nearly 880 geological disasters, resulting in 18 deaths. Currently, there are 2,470 known geological hazard points in Henan Province, threatening 165,200 people and property valued at 6.611 billion yuan. Based on the stage of gully evolution, the geological disaster susceptibility of Henan Province was zoned into four regions. The extremely high susceptibility area is mainly distributed in the mountainous and hilly areas of the Taihang Mountains in northern Henan, the mountainous and hilly areas of the Xiaoshan, Xiong'ershan, Funiu Mountains, Songshan and Wai Fangshan in western Henan, as well as the mountainous and hilly areas of the Tongbai Mountains and Dabie Mountains

in southern Henan. A total of 1,080 small watersheds were delineated, covering a total area of 33,074.51 square kilometers.

Lingbao City[7], a representative geological disaster hotspot in western Henan Province, is located at the southeastern edge of the Loess Plateau. It is bordered by the Xiaoqinling-Xiaoshan Mountains to the south and the Yellow River valley to the north. The region’s high disaster susceptibility arises from the combined effects of three key factors: (1) thick, erosion-prone loess deposits, (2) active tectonic uplift along the Qinling orogenic belt, and (3) extensive mining-induced terrain modifications. This natural-anthropogenic synergy makes Lingbao an ideal model for investigating hazard dynamics within provincial-scale disaster corridors.

2.2 Methods and datasets

In this study, DInSAR and SBAS-InSAR processing were performed using LandSAR software[8, 9], which was developed by the Land Satellite Remote Sensing Application Center (MNR)[10].

Firstly, We utilized 1,763 LT-1 scenes with 3-meter resolution across Henan Province, encompassing 694 ascending-orbit and 1,069 descending-orbit scenes, along with the 30-meter resolution COP-DEM as external DEM data, to perform two-track DInSAR processing. Secondly, to mitigate the impact of noise, atmospheric, and topographic errors on the interpretation of geological disaster information in DInSAR results[11], we utilized the Small Baseline Subset (SBAS)[12] temporal InSAR technique to process 700 scenes of LT-1 data with a 3-meter resolution. This data spanned from July 2023 to July 2024 and focused on the key geological hazard-prone areas of Henan Province, yielding deformation rate field results. Furthermore, we integrated mining area boundaries into our deformation screening method and overlaid optical imagery and topographic data to facilitate a three-dimensional integrated interpretation. This approach allowed us to preliminarily identify the types of geological hazards and gather basic information about the disaster-prone elements during the screening process. The deformation screening work is still in progress. Thirdly, during the deformation screening process, we conducted a detailed investigation and field survey in Lingbao City.

Parameter	DInSAR		SBAS-InSAR	
Band	L			
Wavelength (cm)	23.8cm			
Azimuth/Range pixel spacing	4.65m/1.67m			
Polarization	HH			
Acquisition time	June 2023-July 2024		July 2023-July 2024	
Orbit direction	Ascending	Descending	Ascending	Descending
Number of data	694	1,069	217	483

Table 1. Main parameter of LT-1 and data usage

3. Results and analysis

DInSAR resulted in a total of seven deformation field datasets, identifying a total of 1304 areas of ground deformation, see Fig.1. Only 158 coincident points were found compared to the registered geological disaster points, see Fig.2. The main reasons are: on one hand, registered points are mostly areas where past geological disasters occurred. These areas may not have deformed in this monitoring cycle and thus were not detected. On the other hand, mining-related disasters (e.g., ground subsidence and slope deformation) change with mining locations, so they may not match registered points.

During the deformation screening process, we conducted a detailed investigation and field survey in Lingbao City, identifying 14 new ones.

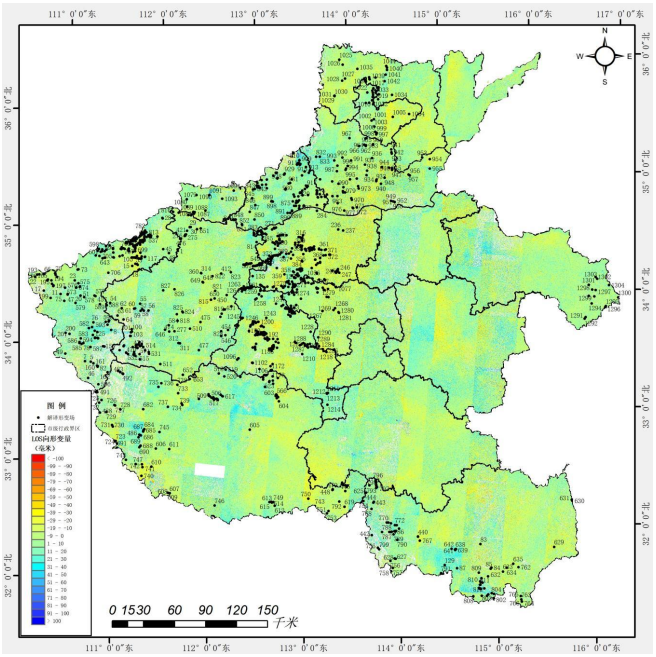

Figure 1. D-InSAR results of Henan province

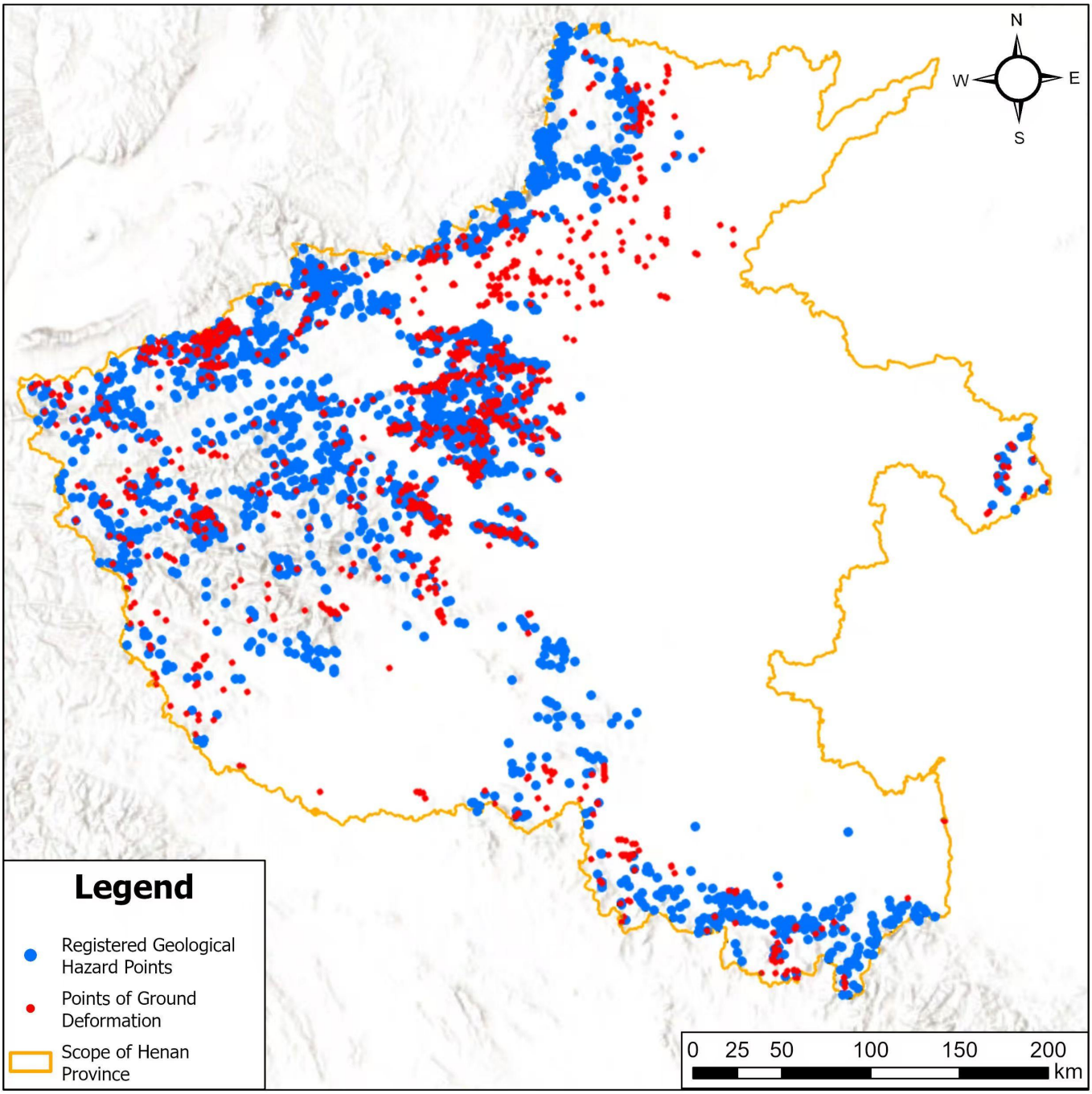

Figure 2.The results comparing with the registered geological disaster points

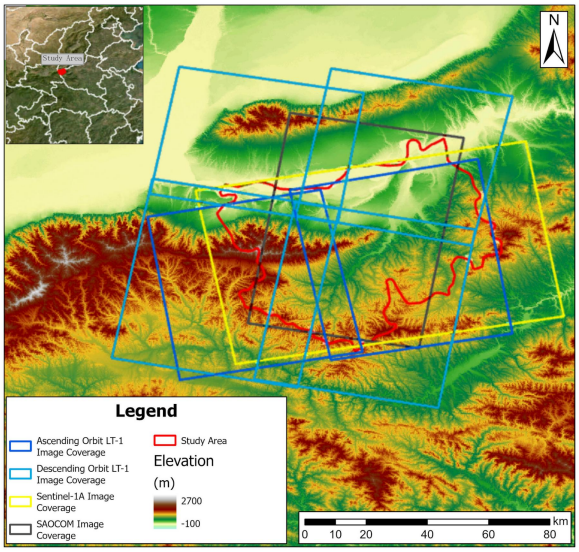

Figure 3. Topographic map of Lingbao City

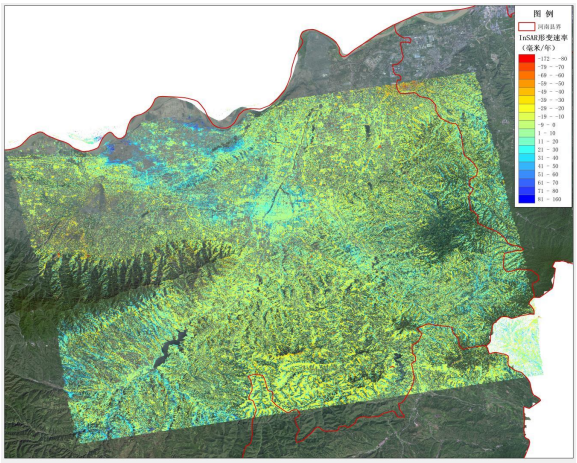

Figure 4. Deformation velocity results of Lingbao city

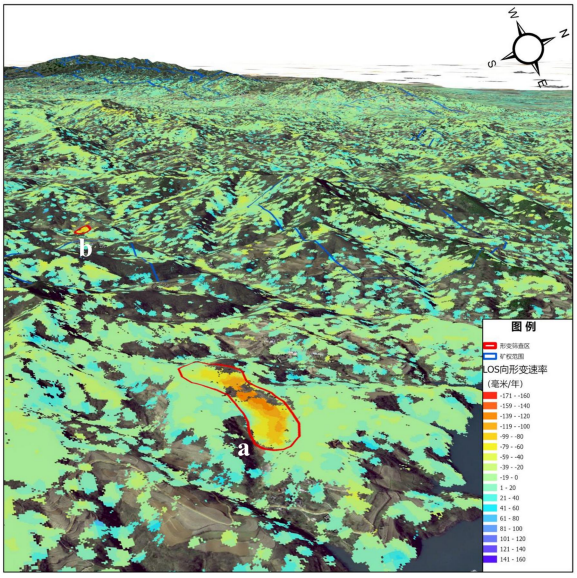

Figure 5. The process of 3D integrated deformation field screening. a is the No. 1 Hazard Point, and b is the No. 13 Hazard Point.

Considering the weather and environmental conditions, in order to confirm the accuracy of SBAS results, we used Unmanned air vehicle (UAV)[13] at Points No. 1 and No. 13 for detailed analysis, given that geological disasters are prone to occur in complex terrains such as mountainous areas[14], steep slopes, and canyons, where transportation is usually inconvenient. Slope No. 1 in Zhouyu Village, Lingbao City, has max deformation of 53.3mm/y LOS, with identifiable rear edge, secondary slide plane, bulge, and fan cracks from LiDAR DEM[15].

Slope No. 13 in Sangyuan Village, Lingbao City, has max deformation of 74.4mm/y LOS, with two traction cracks and an adjacent ancient landslide visible from LiDAR DEM. The ancient landslide boundary is clear in oblique photo models[16]. Located within a gold mine concession[17], the slope movement is attributed to human mining activities affecting geological structures[18].

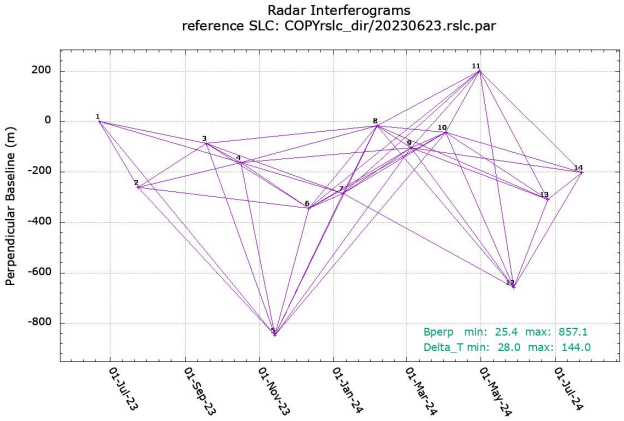

Figure 6. Temporal baseline of No. 1 and No. 13 Hazard Points

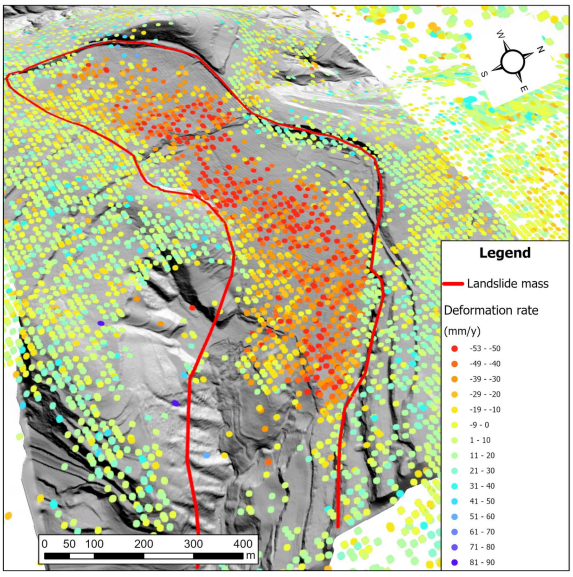

Figure 7. SBAS+ LiDAR DEM of No. 1 Hazard Point

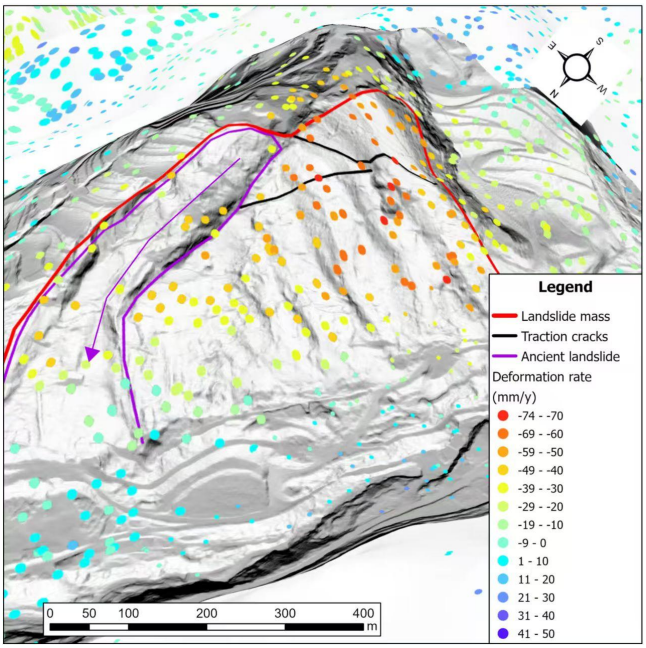

Figure 8. SBAS +LiDAR DEM Overlay Map of No. 13 Hazard Point

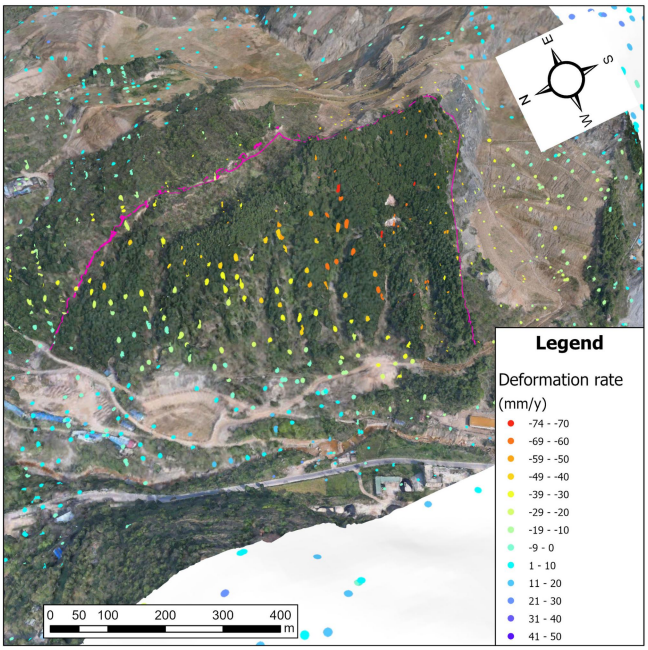

Figure 9. UAV tilt photography of No. 13 Hazard Point

4. Conclusion

This study combines D-InSAR, SBAS-InSAR, and UAV-based LiDAR data to improve geological disaster prediction accuracy. D-InSAR provides initial deformation data, while MT-InSAR offers detailed deformation rates through data stacking to reduce redundancy. UAV LiDAR delivers high-precision terrain data, addressing InSAR limitations in complex terrains. LiDAR data corrects InSAR terrain errors, and MT-InSAR reduces atmospheric delay errors. The combination of UAV LiDAR's flexibility and InSAR's wide-area monitoring enhances real-time monitoring efficiency.

5. Acknowledgement

This work was supported by National Key R&D Programme of China (2023YFB3904905).

6. References

R. Tomás and Z. Li, "Earth Observations for Geohazards: Present and Future Challenges," Remote Sensing, vol. 9, p. 194, 2017.

Q. Xu, "Understanding and Consideration of Related Issues in Early Identification of Potential Geohazards," Geomatics and Information Science of Wuhan University, vol. 45, pp. 1651-1659, 2020.

X. H. Zhou B, Wen G., "The susceptibility zoning of rainfall - type geological hazards in Henan Province based on erosion cycle theory[J]," Journal of North China University of Water Resources and Electric Power (Natural Science Edition), vol. 45(4), pp. 92-101, 2024.

L. Zhang, K. Dai, J. Deng, D. Ge, R. Liang, W. Li, et al., "Identifying Potential Landslides by Stacking-InSAR in Southwestern China and Its Performance Comparison with SBAS-InSAR," Remote Sensing, vol. 13, p. 3662, 2021.

K. L. ROBERT WANG , DACHENG LIU, NAIMING OU , HAIXIA YUE, YAFENG CHEN, WEI YU, DA LIANG , AND YONGHUA CAI, "LuTan-1_An_innovative_L-band_spaceborne_bistatic_interferometric_synthetic_aperture_radar_mission," IEEE GEOSCIENCE AND REMOTE SENSING MAGAZINE, 2024.

T. Li, X. Tang, X. Zhou, X. Zhang, S. Li, and X. Gao, "Deformation Products of Lutan-1(LT-1) SAR Satellite Constellation for Geohazard Monitoring," presented at the IGARSS 2022, Kuala Lumpur, Malaysia, 2022.

L. N. R. a. P. Bureau., "Lingbao Natural Resources and Planning Bureau Announces Existing Geological Disaster Hazard Points.," ed, 2024.

J. Lu, X. Zhou, T. Li, X. Zhang, X. Zhang, T. Li, et al., "LandSAR Software Testing Method For LuTan-1 SAR Standard Product Generation In Natural Resource Monitoring," presented at the IET International Radar Conference (IRC 2023), Chongqing, China, 2023.

J. Lu, X. Zhou, X. Zhang, X. Zhang, and L. Hu, "Big Data Oriented InSAR Software Testing Method For LandSAR Used In Chinese Satellite Lutan-1 Applications," presented at the SAR In Big Data Era, Beijing,China, 2023.

T. Li, T. Li, X. Zhou, J. Lu, X. Zhang, X. Zhang, et al., "An InSAR Processing Software Development and Management Method using Model-View-Controller Design Mode: LandSAR," in SAR in Big Data Era, Beijing, China, 2023.

Y. Xu, T. Li, X. Tang, X. Zhang, H. Fan, and Y. Wang, "Research on the Applicability of DInSAR, Stacking-InSAR and SBAS-InSAR for Mining Region Subsidence Detection in the Datong Coalfield," Remote Sensing, vol. 14, p. 3314, 2022.

F. Casu, M. Manzo, A. Pepe, and R. Lanari, "SBAS-DInSAR analysis of very extended areas: First results on a 60000 km2 test site," IEEE Geoscience and Remote Sensing Letters, vol. 5, p. 438 −442, 2008.

D. P. S. Bekaert, C. E. Jones, K. An, and M.-H. Huang, "Exploiting UAVSAR for a comprehensive analysis of subsidence in the Sacramento Delta," Remote Sensing of Environment, vol. 220, pp. 124-134, 2019.

Y. Zheng, Z. Chen, and G. Zhang, "Application and Evaluation of the Gaofen-3 Satellite on a Terrain Survey with InSAR Technology," Applied Sciences, vol. 10, p. 806, 2020.

F. Hu, F. J. v. Leijen, L. Chang, J. Wu, and R. F. Hanssen, "Monitoring Deformation along Railway Systems Combining Multi-Temporal InSAR and LiDAR Data," Remote Sensing, vol. 11, p. 2298, 2019.

S. Y. DAl Keren, WU Mingtang, et al, " ldentification of potential landslides in Baihetan Dam area before theimpoundment by combining InSAR and UAV survey," Acta Geodaetica et Cartographica Sinica, vol. 51(10), pp. 2069-2082, 2022.

M. Ilieva, P. Polanin, A. Borkowski, P. Gruchlik, K. Smolak, A. Kowalski, et al., "Mining Deformation Life Cycle in the Light of InSAR and Deformation Models," Remote Sensing, vol. 11, p. 745, 2019.

Y. Ji, X. Zhang, T. Li, H. Fan, Y. Xu, P. Li, et al., "Mining Deformation Monitoring Based on Lutan-1 Monostatic and Bistatic Data," Remote Sensing, vol. 15, p. 5668, 2023.